High Rate Capability of Carbon Nanofilaments with Platelet Structure as Anode Materials for Lithium Ion Batteries

H. Habazaki*, M. Kiriu and H. Konno

Graduate School of Engineering, Hokkaido University, N13-W8, Sapporo 060-8628, Japan

*Corresponding author: Phone and fax, +81-11-706-6575; e-mail,

habazaki@eng.hokudai.ac.jp

Abstract

Carbon nanofilaments (CNFs) with platelet structure have been prepared by liquid phase carbonization using porous anodic alumina template, and their lithium ion insertion/extraction properties have been examined as a function of heat treatment temperature and filament diameter. The CNFs heat-treated at 1000°C reveal higher capacitance and higher rate capability compared with those heat-treated at higher temperatures. Further, it is found that higher reversible capacity is obtained for the CNFs with reduced diameter. The reversible capacity of highly graphitized CNFs formed at 2800°C is less than 200 mA h g^{-1} at a current density of 50 mA g^{-1}, being far lower than the theoretical capacity (372 mA h g^{-1}) of graphite. A probable reason is the presence of loop at the edge of graphene layers.

Keywords: carbon nanofilaments, platelet structure, lithium ion battery, rate capability, intercalation reaction

1. Introduction

Lithium ion batteries are currently used in a range of portable electronic devices, including mobile phones, laptop computers and video cameras, due to their high energy density. To expand the application fields of lithium ion batteries to automotive industry, there is a need to improve the rate capability of the batteries to get high power density. It is widely believed that the limitations of rate capability of lithium ion batteries result from slow solid state diffusion of lithium ions in the active electrode materials [1]. Thus, increasing interest is directed toward nanostructured electrode materials since the nanostructure reduces clearly the distance that lithium ions must diffuse. Martin and his co-workers demonstrated the improved rate capabilities of nanostructured SnO_2 and V_2O_5 electrodes, prepared by a template method, relative to the corresponding thin film controlled electrodes [2-7]. They have also reported

that nanostructured honeycomb carbon anode delivers 50 times the capacity of the thin film-controlled anode that does not have honeycomb nanopores [8]. From these results, they have concluded that the improved rate capability is associated with shorter solid state diffusion path in the nanostructured materials.

Carbonaceous materials have been used predominantly as an anode in commercial lithium ion batteries. Thus, nanostructured carbon materials have attracted increased attention as an anode for high power applications [9, 10]. Recently, some of the present authors have prepared platelet structure carbon nanofilaments (CNFs) by liquid phase carbonization in pores of porous anodic alumina templates [11]. Since pore size of the template can be controlled by changing anodizing conditions, such as electrolyte and formation voltages [12], CNFs with different diameters can be prepared readily. Furthermore, platelet structure is developed even at temperature as low as 600°C, with the graphitization degree increasing with heat treatment temperature. The CNFs thus prepared, therefore, allow us to examine systematically the influence of the diameter of the CNFs and graphitization degree on the anode characteristics of lithium ion batteries. In the present study, the charge/discharge characteristics of the CNFs prepared by the template technique have been examined with a particular attention paid to the rate capability of the CNFs of different diameters and with different crystallization degrees.

2. Experimental

A template of porous anodic alumina films of about 30 nm in pore diameter was prepared by anodizing high purity aluminium foil at 25 V in 0.3 mol dm^{-3} sulphuric acid electrolyte for 2 h, and subsequent pore widening in 5% phosphoric acid solution at room temperature for 30 min. This template was used without removing aluminium metal substrate and a barrier oxide layer at the bottom of the porous alumina layer. A commercial porous anodic alumina

membrane filter (Whatman, Anodisc-25) was also used as a template of approximately 230 nm in pore diameter.

A mixture of the porous alumina template and polyvinyl chloride (PVC) powders (TK-500, Shin-Etsu Chemicals Co. Ltd.) was heated in a stream of high purity argon at 400 K h^{-1} to 300^{o}C, and then it was kept at this temperature for 30 min. Around this temperature, PVC decomposes to liquefied pitch-like intermediate, penetrating into pores of the template. Subsequently, it was heated up to 600^{o}C and kept for 1 h. Then, the template was dissolved in 10% NaOH solution and the CNFs formed were filtered. The CNFs were further heat-treated at 1000 or 1500^{o}C for 1 h or 2800^{o}C for 30 min in a stream of high purity argon.

Structure and morphology of the CNFs were examined by a JEOL JSM-6300F scanning electron microscope and a JEOL JEM-2010 transmission electron microscope. The electrochemical lithium insertion/extraction characteristics were studied by charge/discharge measurements using a three electrode cell. The working electrode was prepared by coating a mixture of CNFs and polyvinylidene fluoride (PVDF) (9:1 mass ratio) on a porous nickel sheet. The coated specimen was pressed at about 20 MPa before use. A liquid electrolyte of 1 mol dm^{-3} $LiClO_4$ dissolved in EC + DEC (1:1 volume ratio) was used. Lithium metal sheet was used for both counter and reference electrodes. The charge/discharge measurements were performed in a potential range of 0.003 to 2.5 V vs Li^{+}/Li. By using this procedure, highly reproducible charge/discharge curves were obtained.

3. Results and Discussion

3.1. Structure of CNFs

The CNFs formed from PVC using porous anodic alumina templates have high aspect ratio and their diameters are approximately in agreement with the pore diameters of the respective templates [11]. An example of the carbon nanofibers of average 230 nm in diameter,

heat-treated at 1500°C is shown in Fig. 1. The length of the nanofilaments, generally less than several micrometres, is not as long as the thickness of the template (~50 μm), probably due to fracture of the filaments during heat treatment. Hollow regions, present in the nanofilaments formed at 600°C, may be possible sites of fracture. High resolution transmission electron micrograph, shown in Fig. 1(b), depicts that graphene layers observed are normal to the fibre axis; such orientation is referred to as platelet structure.

The platelet structure is developed irrespective of the diameter of the CNFs. Fig. 2 shows transmission electron micrographs of the CNFs of about 30 nm in diameter, heat-treated at 1000 and 2800°C. The platelet structure is evident at both temperatures, although graphitization proceeds with increasing heat treatment temperature. As shown in Fig. 2(b), loops are developed at the edge of graphene layers, being typical of the CNFs heat-treated at as high as 2800°C [13, 14]. Apparently, adjacent each 4-5 carbon layers are connected by a loop.

3.2. Lithium ion insertion/extraction characteristics

The charge and discharge characteristics of the CNFs of 30 nm in diameter, measured at 50 mA g^{-1} (Fig. 3), are dependent upon the heat treatment temperature. Highly graphitized CNFs formed at 2800°C reveals a potential plateau region at low potential, similar to typical graphite materials, although the reversible capacity (~190 mA h g^{-1}) is far lower than the theoretical capacity of graphite (372 mA h g^{-1}). The irreversible capacity at the first cycle is as large as 377 mA h g^{-1}. The potential plateau region between 0.7-0.9 V vs Li^+/Li found only at the first charge is associated with the decomposition of electrolyte to form the solid electrolyte interphase (SEI) film on the CNFs surface. The irreversible capacity decreases markedly after the second cycle.

The charge-discharge curves for the CNFs heat-treated at 1000 and 1500°C (Fig. 3(a)-(b))

are similar to typical carbon materials with low graphitization degree; the potential changes gradually without showing a plateau region. The irreversible capacities at the first cycle for both the CNFs are as large as that heat-treated at 2800°C, probably due to similar surface area of these specimens. The reversible capacity is largest for the CNFs formed at 1000°C and that formed at 1500°C is nearly the same as that formed at 2800°C. The values for the CNFs formed at 1000 and 1500°C are in agreement with those of typical soft carbon materials reported previously [15]. In contrast, the CNFs formed at 2800°C reveals far lower reversible capacity compared with the soft carbon materials heat-treated at the same temperature (~300mA h g^{-1}) [15]. The low capacity of the CNFs formed at 2800°C is probably associated with the presence of loops at the edge of graphene layers. The loops may impede the intercalation of lithium ions into all of interlayers in the CNFs.

The beneficial effect of the reduced diameter of CNFs on the capacity can be found from the charge/discharge cycle performance shown in Fig. 4. The result of carbonaceous materials formed from PVC at 1000°C without template is also shown for comparison. In this experiment the current density increased every 5 cycles. Except the first 5 cycles, during which the reversible capacity decreases gradually, the relatively stable capacity is obtained at each current density. It is evident from the figure that the reversible capacity of the CNFs with smaller diameter is larger at all the current densities examined. Fig. 5 shows the reversible capacity of the CNFs relative to that at 50 mA g^{-1} as a function of current density. Obviously, the CNFs formed at lower temperature reveals higher rate capability.

The repeated insertion and extraction of lithium ions is likely to deteriorate the cycle performance of the platelet structure CNFs with small diameter due to exfoliation. However, when the cycle performance of the CNFs with 30 nm in diameter formed at 1000°C was examined at a current density of 100 mA g^{-1}, rather stable capacity was confirmed at least up to 85 cycles. The decrease in capacity was found mainly at initial several cycles as in Fig. 4.

Only the disadvantage of the platelet CNFs with small diameter is the large irreversible capacity at the first cycle. The large edge surface of graphene layers for the CNFs results in the formation of a large amount of SEI film. In fact, it was found that the irreversible capacity at the first cycle increases with a decrease in the diameter of the CNFs. Since suitable additives in electrolytes have been found recently to form only a thin the SEI film and to reduce the reversible capacity [16], a reasonable reduction of the irreversible capacity of the platelet structure CNFs would be possible. This is the subject of the next step.

4. Conclusions

High rate capability of the platelet structure CNFs, formed from a mixture of PVC and porous anodic alumina template, as anode materials for lithium ion batteries was found for the first time. The better rate capability is obtained when the CNFs are heat-treated at 1000°C; further increase in the heat treatment temperature is detrimental for the anode performance. The rate capability is improved by reducing the diameter of the CNFs.

Acknowledgments

Thanks are due to Professor Y. Kaburagi, Musashi Institute of Technology for the heat treatment of the carbon nanofilaments at 2800°C. The present work was supported in part from the Ministry of Education, Culture, Sports, Science and Technology (Exploratory Research No. 16651053) and Tokuyama Science Foundation.

References

1. P.R. Bueno, E.R. Leite, J. Phys. Chem. B 107 (2003) 8868.
2. C.R. Sides, C.R. Martin, Adv. Mater. 17 (2005) 125.
3. C.J. Patrissi, C.R. Martin, J. Electrochem. Soc. 148 (2001) A1247.

4. N.C. Li, C.R. Martin, B. Scrosati, J. Power Sources 97-8 (2001) 240.

5. N.C. Li, C.R. Martin, J. Electrochem. Soc. 148 (2001) A164.

6. N.C. Li, C.R. Martin, B. Scrosati, Electrochem. Solid State Let. 3 (2000) 316.

7. C.J. Patrissi, C.R. Martin, J. Electrochem. Soc. 146 (1999) 3176.

8. N.C. Li, D.T. Mitchell, K.P. Lee, C.R. Martin, J. Electrochem. Soc. 150 (2003) A979.

9. T. Doi, A. Fukuda, Y. Iriyama, T. Abe, Z. Ogumi, K. Nakagawa, T. Ando, Electrochem. Commun. 7 (2005) 10.

10. E. Frackowiak, F. Beguin, Carbon 40 (2002) 1775.

11. H. Konno, S. Sato, H. Habazaki, M. Inagaki, Carbon 42 (2004) 2756.

12. S. Ono, N. Baba, N. Masuko, J. Surf. Finish. Soc. Jpn. 42 (1991) 133.

13. S. Lim, S.H. Yoon, I. Mochida, J.H. Chi, J. Phys. Chem. B 108 (2004) 1533.

14. G.-B. Zheng, H. Sano, Y. Uchiyama, Carbon 41 (2003) 853.

15. J.R. Dahn, T. Zheng, Y.H. Liu, J.S. Xue, Science 270 (1995) 590.

16. H. Zheng, Y. Fu, H. Zhang, T. Abe, Z. Ogumi, Electrochem. Solid State Let. 9 (2006) A115.

Figure captions

Fig.1 (a) SEM and (b) TEM images, with selected area electron diffraction pattern, of the CNFs of 230 nm in diameter heat-treated at 1500°C.

Fig. 2 TEM images of the CNFs of 30 nm in diameter heat-treated at (a) 1000°C and (b) 2800°C.

Fig. 3 Charge-discharge curves, measured at a current density of 50 mA g^{-1}, of the CNFs of 30 nm in diameter, heat-treated at (a) 1000°C, (b) 1500°C and (c) 2800°C

Fig. 4 Cycle performance of the CNFs of 30 and 230 nm in diameter as well as the carbonaceous material formed without template. All the specimens were heat-treated at 1000°C. Every 5 cycles the current density was increased in the following order: 50, 200, 500, 1000, 1500 and 2000 mA g^{-1}.

Fig. 5 The reversible capacity relative to that at a current density of 50 mA g^{-1} for the CNFs of 30 nm in diameter, heat-treated at 1000, 1500 and 2800°C as a function of the current density.

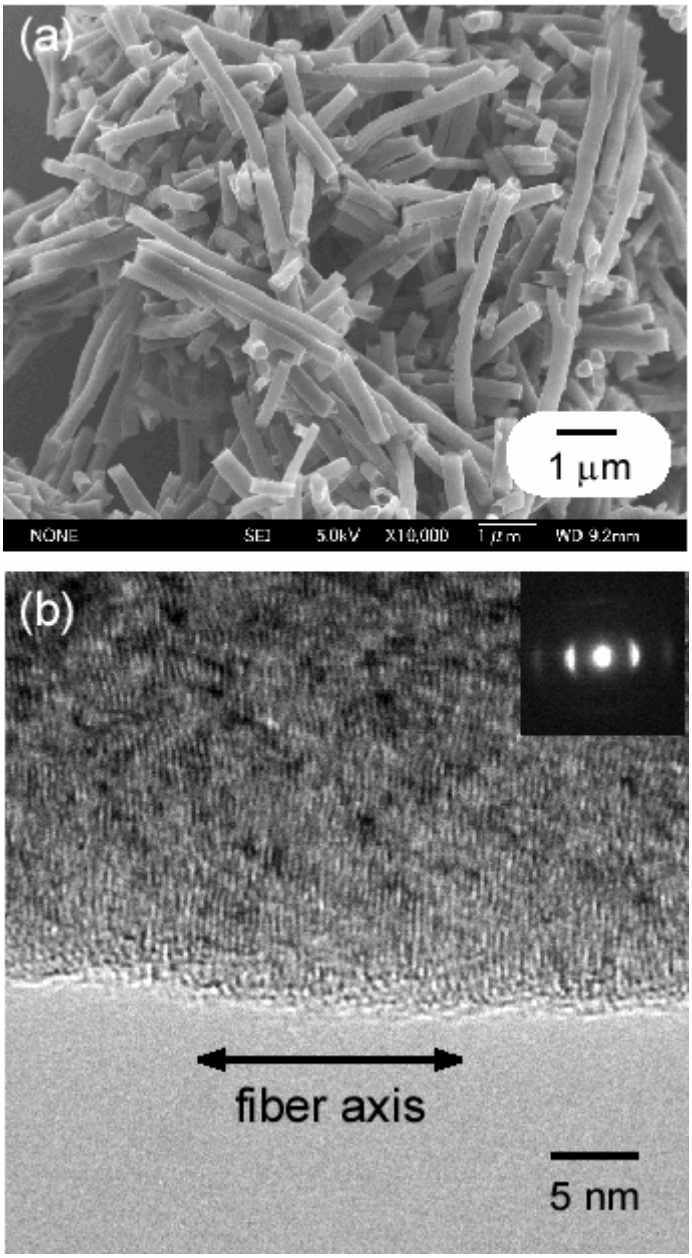

Fig.1 (a) SEM and (b) TEM images, with selected area electron diffraction pattern, of the CNFs of 230 nm in diameter heat-treated at 1500°C.

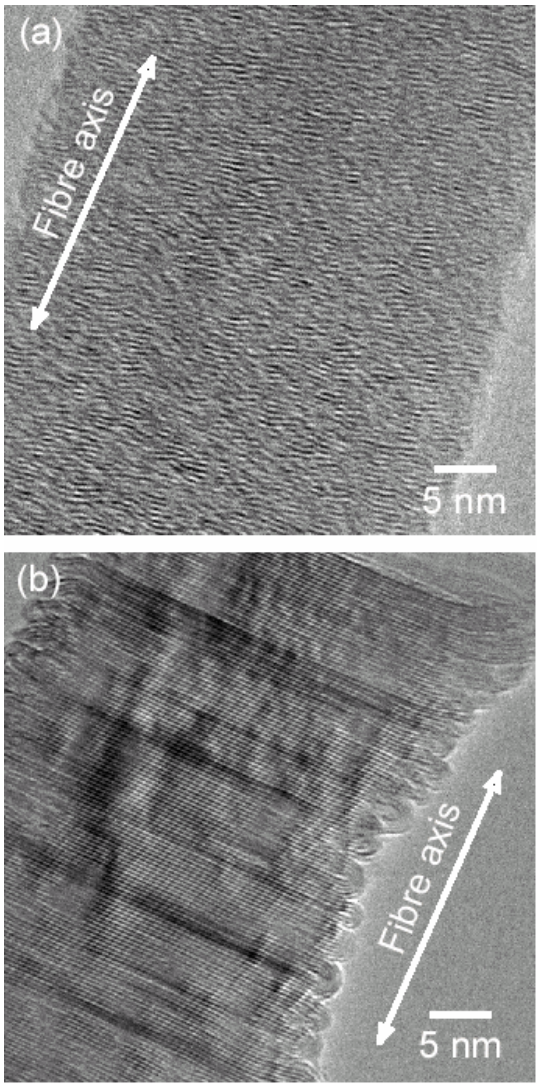

Fig. 2 TEM images of the CNFs of 30 nm in diameter heat-treated at (a) 1000°C and (b) 2800°C.

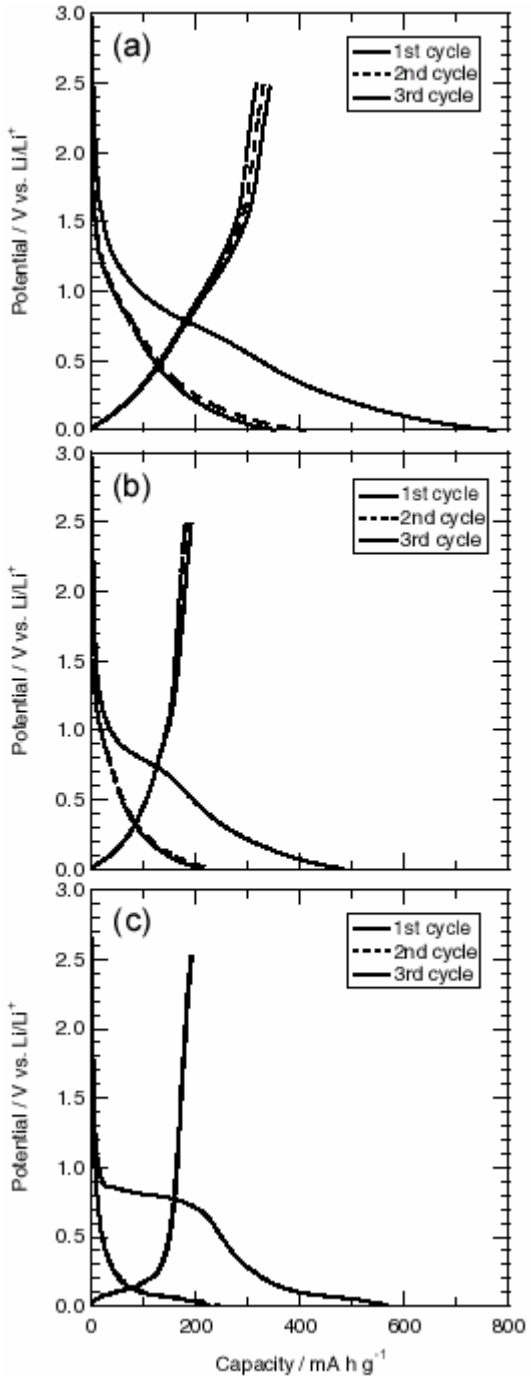

Fig. 3 Charge-discharge curves, measured at a current density of 50 mA g^{-1}, of the CNFs of 30 nm in diameter, heat-treated at (a) 1000°C, (b) 1500°C and (c) 2800°C

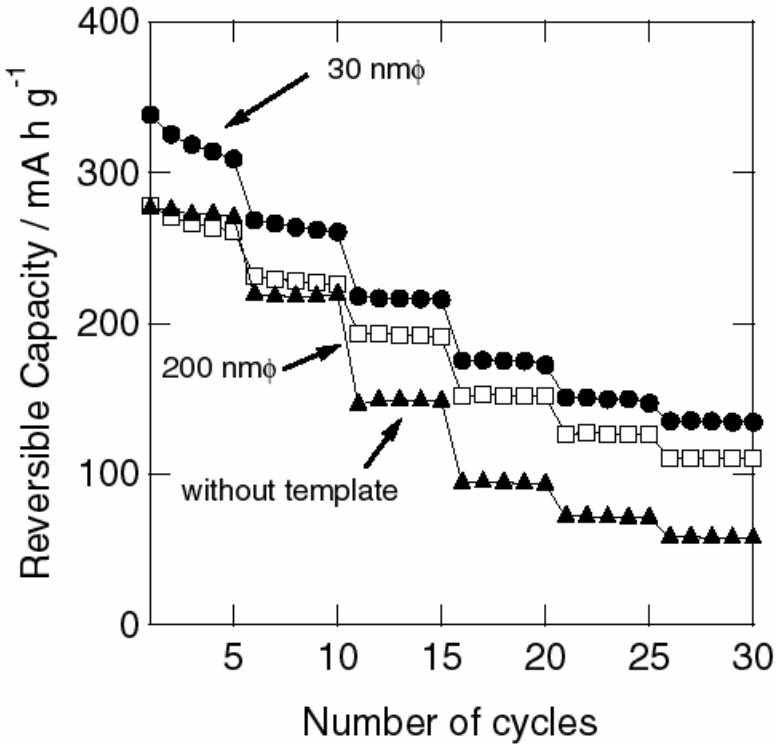

Fig. 4 Cycle performance of the CNFs of 30 and 230 nm in diameter as well as the carbonaceous material formed without template. All the specimens were heat-treated at 1000°C. The current density was increased every 5 cycles in the following order: 50, 200, 500, 1000, 1500 and 2000 mA g^{-1}.

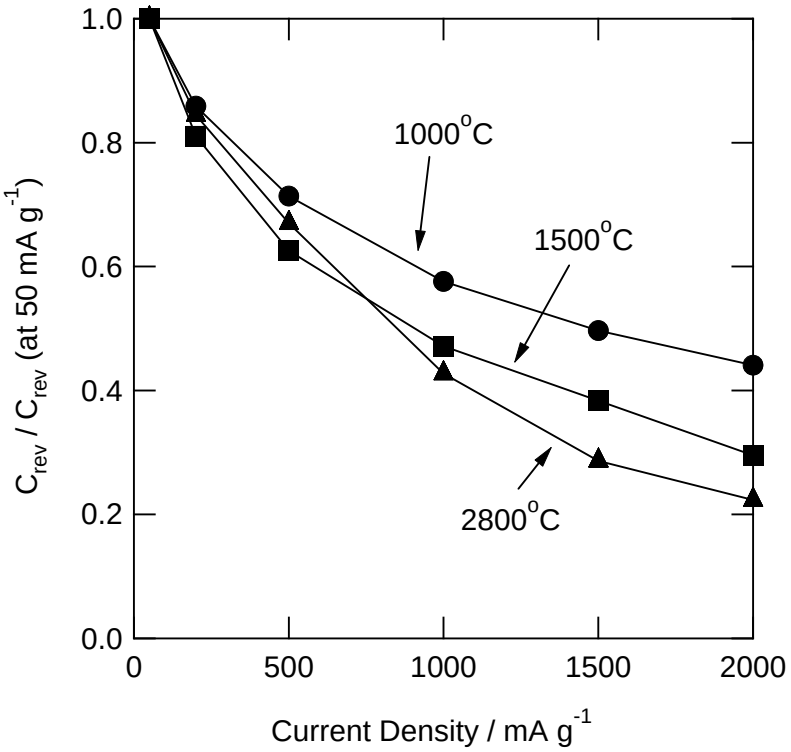

Fig. 5 The reversible capacity relative to that at a current density of 50 mA g^{-1} for the CNFs of 30 nm in diameter, heat-treated at 1000, 1500 and 2800°C as a function of the current density.